International Journal of Hydraulic Engineering 2013, 2(5): 101-114
DOI: 10.5923/j.ijhe.20130205.04

Turbulence Measurements above Sharp-crested Gravel Bedforms

Elham Nasiri Dehsorkhi[1,*], Hossein Afzalimehr[1], Jacques Gallichand[2], Alain N Rousseau[3]

[1]Department of Water Engineering, Isfahan University of Technology, Isfahan, Iran
[2]Department des sols et de génie agroalimentaire, Pavillon Paul-Comtois, Université Laval, St-Foy, QC, Canada
[3]Institut National de la Recherche Scientifique, Centre Eau Terre Environnement, Québec City, QC, Canada, G1K 9A9

Abstract This paper primarily presents velocities, Reynolds stresses and turbulence intensities of flow over a series of two-dimensional asymmetric sharp-crested, gravel bedforms. The bedforms have a mean wavelength of 0.96 m, a mean height of 0.08 m, and a width of 0.4 m (equal to the flume width) and a lee slope of 28°. The results show that extrapolating spatially-averaged log-law velocity profiles provided the best estimate of bed shear stress for bedforms. Maximum values of the root-mean-squared velocity over the sharp-crested gravel bedforms were located farther away from the bed when compared to those for sand dunes. The Reynolds stresses were zero or negative near the water surface over sand dunes, whilst they were positive over sharp-crested gravel bedforms. The length of the separation zone of gravel dunes was less than that for sand dunes, showing a faster reattachment over a gravel bed in comparison to that of a sand bed. Quadrant analysis showed that near the bed the contributions of sweep and ejection events changed with an oscillatory pattern along the sharp-crested gravel bedforms, however, such a pattern was not observed close to the water surface.

Keywords Gravel Bedforms, Turbulence, Flow Separation, Reynolds Stress, Quadrant Analysis

1. Introduction

Gravel and sand bedforms occur locally in rivers and can be found in regions characterized by small, to moderate, sediment transport rate and relatively high-energy conditions. The effect of gravel and sand bedforms on a turbulent flow is important in determining friction factor and sediment transport in coarse-bed rivers. These bedforms arise from the interactions of the coarse bed with the flow, revealing considerable changes in the mean flow and turbulence characteristics. The spatial evolution of the turbulence field over gravel and sand bedforms is dominated by flow separation and reattachment processes along with wake formation. Several investigations have provided insights on the influence of gravel and sand bedforms on their associated turbulent flow features ([1],[2],[3]). Most of the data on gravel bedforms come from studies conducted by Dinehart ([4],[5],[6]).

However, Carling[2] investigated bedforms with *D/L* ratios (*D*, dune height; *L*, dune length) in both gravel and sand dunes. He stated that the height of gravel bedforms should reach an equilibrium value equivalent to that for sand dunes. However, owing to the particular constraints of experimental and field conditions, data for gravel bedforms have often pertained to non-equilibrium and/or depth-limited conditions. For example, most of *D/L* ratios for gravel bedforms reported in the literature have had a tendency to be low, and rarely commensurate with equilibrium values recorded for deep-water, sand-dune trains ([5],[6]).

The flow over a two-dimensional bedform is highly non-uniform, accelerating over the bedform, upstream slope due to convergence, and decelerating over the bedform trough due to expansion. In general, bedform formation causes flow separation at the crest, creating a large recirculation zone on the leeside of the bedform. The flow reattaches approximately four to six bedform heights downstream of the crest[7]. Downstream of the point of reattachment, a new boundary layer develops and grows as the flow accelerates towards the next bedform crest. This flow structure induces a high pressure region downstream of the reattachment point, upstream of the next bedform, and a low pressure region on the steep lee side, so on and so forth.

Bennett and Best[1] investigated using a laboratory flume velocity and turbulence structures over fixed, two-dimensional sand dunes (grain diameter 0.3 mm), having a length of 0.63m, a height of 0.04m and a lee angle of 30° in a laboratory flume. They used ratios of wavelength/flow depth of 4-5, wavelength/bedform height of 15-17 and flow depth/bedform height of 2-9; and found considerable symmetry in streamwise and vertical velocities from crest to crest. They also observed that: (i) the maximum streamwise turbulence intensity (root-mean-squared velocity fluctuations) occurred within the flow separation zone and

* Corresponding author:
e.nasiri@ag.iut.ac.ir (Elham Nasiri Dehsorkhi)
Published online at http://journal.sapub.org/ijhe

downstream of the reattachment point, (ii) the maximum vertical turbulence intensity occurred along the shear layer within and above the flow separation zone; and (iii) the maximum Reynolds stresses occurred within the separation zone along the shear layer. Their quadrant analysis showed that ejection events, dominated the shear stress contribution along the local shear layer, and sweep events played a significant role near the reattachment point and close to the dune crest.

Williamson et al.[8] found that two types of dunes developed in the Fraser River estuary, Canada: (i) symmetric dunes with stoss and lee sides of similar lengths, gentle lee side slope angles and rounded crests; and (ii) asymmetric dunes with superimposed small dunes on their stoss sides, and sharp crests with steeper lee sides.

Sharp-crested bedforms were investigated using airflow by Frank and Kocurek[9], Walker and Nickling[10]. However, typical bedform shapes found in rivers are rounded crest, i.e. where the brink is clearly distinguishable from the crest. Tsoar[11] showed that the rounded dunes were more stable than those that are triangular, since the sharp-crested shape experienced strong flux at the brink. Sharp-crested bedforms usually develop from the strongly increased gravel drift close to the crest, operating in horizontal and vertical directions, and may change with flow direction. To present a realistic model, showing flow structure over bedforms before forming a round crest which are typically observed in rivers, it is required to understand the flow structure over a triangular-crested bedform. To corroborate results of CFD simulations (computational fluid dynamics of Reynolds-averaged Navier-Stokes equations) or perhaps provide modeling insights to large eddy simulation (LES) models of flows over sharp-crested gravel bedforms, there is a need to investigate these shapes in details in the laboratory. This represents the primary of objective of this paper.

More specifically, this study: (i) investigated the characteristics of the velocity fields, Reynolds stresses, and turbulent intensity distributions, using accurate and detailed measurements over sharp-crested, gravel bedforms set in a laboratory flume, and (ii) compared the ensuing results with those reported by Bennett and Best (1995) in their study on flows over sand-bed dunes. Furthermore, the following questions were addressed: (i) What is the effect of sharp-crested gravel dunes on velocity and Reynolds stress distributions?; (ii) How does the separation length change over gravel bedforms with respect to that observed for sand-bed dunes?; (iii) What are the dominant events of the bursting process over sharp-crested bedforms?; and (iv) How do the dominant events over gravel bedforms change when compared to those characterizing sand bedforms?

2. Experimental Setup

The experiments were conducted using a re-circulating flume of the Hydraulics Laboratory at the Isfahan University of Technology, Iran. The channel was 8-m long, 0.4-m wide and 0.6-m deep with a horizontal longitudinal bottom slope. The walls and base of the flume were made of glass. A gate located at the downstream end controls the water depth in the flume. For all the dunes, the mean flow depth (h) was kept constant at 20 cm, which is defined as the vertical distance between the water surface and the sediment bed at the crest section. The experiments were performed with a discharge, Q, of 0.024 m^3/sec. An electromagnetic current-meter with a digital system was fitted in the inlet pipe to facilitate continuous monitoring of the discharge.

Seven, two-dimensional, fixed bedforms were attached to the bottom of the flume (Figure 1). The bedforms were prepared with well-sorted gravel particles with a median diameter, d_{50}, of 10-mm. The geometric standard deviation, σ_g, of the particle size distribution of the bed sediments, given by $(d_{84}/d_{16})^{0.5}$, was 1.23. The particle sizes were collected from gravel-bed rivers in the central part of Iran where many coarse-bed rivers can be found.

Figure 1. Experimental Set up

To construct the bedforms in hydraulic laboratory, a field investigation was conducted within coarse-bed rivers in central Iran. Based on topographic surveying, the bedform height was taken to be equal to average heights of all dunes within a selected reach, while the length of dunes was set approximately equal to reach length divided by the number of bedforms in the reach. A triangular wooden frame was used to generate bedform shapes in the flume. Two-dimensional bedforms had fairly regular spacing, heights and lengths. The bedforms had a mean wavelength, λ, of 0.96 m and mean height, D, of 0.08 m. The lee slope angle was 28°, and each bedform spanned the entire width of the flume. The lee slope angle was of the order of that of repose of the sediments.

Velocity measurements were conducted using a three-dimensional down-looking Acoustic Doppler Velocimeter (ADV), developed by NORTEK (www.nortec-as.com/en/products). The ADV is a high-precision instrument that measures all three components of the velocity, 5 cm below the probe. The flow field was practically undisturbed by the probe. Factory calibration of the ADV is specified to be ±1.0%. The sampling frequency was fixed at 200 Hz,

block averaging of the entire record (or selected portions) was done using the software WinADV software (www. usbr. gov/ pmts/ hydraulics_lab /twahl/ winadv/). For the vast majority of the tests, the signal-to-noise ratio (SNR), an indication of the sufficiency of seeding material, exceeded the manufacturer's recommended value of 15 db for high-resolution measurements. A correlation coefficient, output with each ADV sample, is a quality parameter that indicates the degree to which all particles within the sampling volume are moving in precisely the same manner. Low values may result from high turbulence, the presence of large individual particles or bubbles, a low SNR, or interference from boundaries. To filter ADV data, four methods were considered including acceleration threshold filter, maximum/minimum threshold filter, SNR/Correlation filter and phase-space. However, only the latter was used in this study. WinADV was used to remove possible aliasing effects and to process the velocity and turbulence data. Data with an average correlation coefficient less than 70% and average SNR less than 15 dB were filtered out.

Sixteen vertical velocity profiles were measured near the flume centerline over one bed form wavelength (between the fifth and sixth bedform crests with numbering starting at the most upstream bedform, in a series of seven two-dimensional bedforms). For each profile, simultaneous streamwise and vertical velocities were collected at 25 to 35 points. At each point, the flow was sampled for 120 s -experience revealed this duration for sampling was adequate for determining accurate turbulence statistics- with the lowest point in each profile being 3 mm above the bed.

The number of bedforms was sufficient for studying the wake and boundary layer characteristics of the flow. Achievement of a quasi-equilibrium flow over the fixed bedforms required adjustment of both the discharge pump (using an electromagnetic flow meter) and the gate opening, while maintaining the correct mean flow velocity and water depth over successive bedform crests. The equilibration condition was accepted when the appropriate mean flow velocity was achieved and the water depth over seven consecutive bedform crests was within ±2 mm. In addition, equilibrium can be defined as the point where the crest profiles appear to be identical, even if this was usually difficult to quantify.

Table 1 shows that rough turbulent flow conditions were achieved in this study. Indeed, for the the sharp-crested gravel bedforms, the Reynolds numbers, Re, were 5.697×104 at the crest and 5.983×104 at the stoss ($Re=4UR_h/\nu$, with R_h, the hydraulic radius (m), U, the flow velocity (m.s^{-1}), and ν, the kinematic viscosity (m^2.s^{-1})). Using extrapolated, spatially-averaged Reynolds stress profiles, the mean bed shear stress was estimated over bedforms. The Froude number, Fr, ($=U/\sqrt{gh}$) were less than unity (0.18 at the crest and 0.12 at the stoss), indicating subcritical flow.

The time-averaged stream-wise velocity, $\overline{u}$, spanwise mean velocity, $\overline{v}$, vertical mean velocity, $\overline{w}$, stream-wise turbulence intensity, $\sqrt{\overline{u'^2}}$, spanwise turbulence intensity, $\sqrt{\overline{v'^2}}$, and vertical turbulence intensity, $\sqrt{\overline{w'^2}}$, were defined as:

$$\overline{u}=\sum_{i=1}^{N}\frac{u_i}{N},\ \overline{v}=\sum_{i=1}^{N}\frac{v_i}{N},\ \overline{w}=\sum_{i=1}^{N}\frac{w_i}{N} \tag{1}$$

$$\sqrt{\overline{u'^2}}=\sum_{i=1}^{N}\sqrt{\frac{(u_i-u)^2}{N-1}},$$

$$\sqrt{\overline{v'^2}}=\sum_{i=1}^{N}\sqrt{\frac{(v_i-v)^2}{N-1}}, \tag{2}$$

$$\sqrt{\overline{w'^2}}=\sum_{i=1}^{N}\sqrt{\frac{(w_i-w)^2}{N-1}}$$

N, which was the number of time series values, equaled 24000 in this study.

The time-averaged local Reynolds shear stress at a point was determined using

$$\tau=-\rho\overline{u'w'} \tag{3}$$

where

$$\overline{u'w'}=\sum_{i=1}^{N}\sqrt{\frac{(u_i-\overline{u})(w_i-\overline{w})}{N-1}} \tag{4}$$

In the above expressions, the prime denotes velocity fluctuations and ρ, water density.

Table 1. Summary of hydraulic conditions and bedform morphology used in this study and study of Bennett and Best (1995)

	Sharp-crested gravel bedform	Bennett and Best (1995)
Flow depth, h (cm)	20 (crest) 28 (stoss)	10 (crest) 12 (stoss)
Mean velocity, U (m.s^{-1})	0.25 (crest) 0.20 (stoss)	0.57 (crest) 0.49 (stoss)
Aspect ratio, W/h	1.96 (crest) 1.52 (stoss)	3 (crest) 2.5 (stoss)
Froude number, Fr	0.18 (crest) 0.12 (stoss)	0.58 (crest) 0.46 (stoss)
Reynolds number, Re ×10^4	5.697 (crest) 5.983 (stoss)	6.291 (crest) 6.490 (stoss)
Shear velocity, u* (m.s^{-1})	0.015	0.025
Dune height, H (cm)	8	4
Dune wavelength, λ (cm)	9	63
Dune height-to-wavelength ratio, H/λ	0.083	0.063
Leeside angle, (in degrees)	28	30

It should be noted that many methods to estimate the bed shear stress, including the Reynolds stress, were investigated in this study but they did not all work well. No theoretical study exists to describe that which part of the Reynolds stress should be used to estimate the bed shear stress when the flow is not uniform (e.g., over bedforms). Therefore, the state-of-the-art method is still rather empirical, and one really cannot be certain if one method is superior to another. The spatially-averaged method provides some advances for

studying flow over irregular boundaries ([12],[13]). The spatially-averaged profiles near the bed do not reflect the average skin friction stress because they are strongly influenced by the wake, as shown by Nelson et al.[14] and the spatially-averaged profiles away from the bed do not reflect the total boundary shear stress because the strong spatial acceleration of the flow affects the coupling between stress and velocity throughout the flow in a manner that cannot be averaged out. The only exception to the latter point is the case when the flow is deeper than the scale of the bed forms, so they truly act as roughness elements[15]. Therefore, using extrapolated, spatially-averaged, log-law velocity profiles provides a meaningful and defendable estimate of the mean boundary shear stress over the entire dune shape which is used in this study.

The angle of the bedform leeside slope was selected near the angle of repose of sediments. The mean height, wavelength, steepness, and cross section of the bedforms were chosen based on the feasibility of experiments in the hydraulic laboratory. However, based on our hypotheses, we could not find any data to investigate the mean velocity, Reynolds stress and turbulence intensity distributions for sharp-crested gravel bedforms. Therefore, the experimental results of Bennett and Best (1995) were used for comparing the results. Table 1 introduces a summary of hydraulic conditions for all experimental investigations.

3. Quadrant Analysis

The bursting events were quantified by the conditional statistics of the velocity fluctuations (u' and w'). It is customary to plot u' and w' according to quadrant in the $u'w'$-plane[16]. To differentiate the larger contributions to $-\overline{u'w'}$ from each quadrant leaving the smaller u' and w' corresponding to more quiescent periods, a hole size parameter H is introduced[17]. The hyperbolic hole region is determined by the curve $|u'w'| = H(\overline{u'u'})^{0.5}(\overline{w'w'})^{0.5}$. Hence, a clear distinction was possible between strong events and weak events for a small-size hole and by taking into account only strong events for a large-size hole. The turbulent events were defined by the four quadrants as outward interactions (i = 1; $u' > 0$; $w' > 0$), ejections (i = 2; $u' < 0$; $w' > 0$), inward interactions (i = 3; $u' < 0$; $w' < 0$), and sweeps (i = 4; $u' > 0$; $w' < 0$). The hole size $H = 0$ implicated that all u' and w' were included. The quadrant analysis revealed the fractional contributions to $-\overline{u'w'}$ from bursting events. At any point in a stationary flow, the contribution to the total Reynolds stress from quadrant i, excluding a hyperbolic hole region of size H, is

$$\langle u'w' \rangle_{i,H} = \lim_{T\to\infty} \frac{1}{T} \int_0^T u'(t)\, w'(t)\, I_{i,H}\, dt \qquad (5)$$

where the angle brackets denote the conditional average while the indicator function $I_{i,H}$ obeys:

$$I_{i,H}(u',w') = \begin{cases} 1 & if\ (u',w') \in i\text{th quadrant and } |u'w'| \geq H|\overline{u'w'}| \\ 0 & otherwise. \end{cases} \qquad (6)$$

Here H is the threshold parameter in the Reynolds stress signals, which enabled us to extract those values of $u'w'$ from the whole set of data, which were greater than H times $|\overline{u'w'}|$ value. The stress fraction of the ith quadrant was defined as:

$$S_{i,H} = \frac{\langle u'w' \rangle_{i,H}}{\overline{u'w'}} \qquad (7)$$

Here, $S_{i,H} > 0$ when i=2 and 4 (Q_2 and Q_4), and $S_{i,H} < 0$ when i=1 and 3 (Q_1 and Q_3). Hence, at a point, the sum of contributions from different bursting events was unity, showing that $\sum_{i=0}^{i=4} [S_{i,H}]_{H=0} = 1$.

To show a measure of relative dominance of sweeping and ejection events, the following relation was introduced:

$$S_H = \frac{S_{2,H}}{S_{4,H}} \qquad (8)$$

4. Results

4.1. Mean Flow Field

Figure 2a shows the measured velocity distribution over a two-dimensional sharp-crested bedform. The data clearly show how the flow separated at the crest and reattached at some point downstream on the next bedform which similar to the flow separation over sand dunes in the study of Bennett and Best (1995) (Figure 2b). This separation created a positive pressure gradient that induced a smaller velocity gradient with the smaller velocity occurring near the bed. The reduction in velocity in the presence of the positive pressure gradients is observed in Figures 2a, 2b. The vertical profiles of the mean values of the stream-wise velocity in Figures 2a, b and the contour maps of the full flow field in Figures 3a, b illustrate the flow characteristics over one bed form. The stream-wise mean velocity profile at the trough position has an inflexion point near the bed resulting from local flow instability. The largest downstream velocity (0.28 $m.s^{-1}$) occurred just upstream of the bedform crest at z/h=0.58, which is in good agreement with published data from sand dune studies ([1],[14]).

Figures 3a and 3b clearly indicate the occurrence of separation and flow reversal as water flows over a bedform. Some studies have revealed that in flow over bedforms, a definitive region of momentum defect could be observed ([1],[14]) which is related to flow separation and the wake formation downstream of the bedform lee face. As the wake is advected downstream, the influence of the momentum defect is diffused outward, forcing the region to grow in depth[18]. Moreover, the length of flow separation, X_r, was measured from the crest, where the flow separates, to the

flow reattachment point. The reattachment point was determined by observing the horizontal velocity component in the lee of the bedform. The reattachment point is located where the horizontal velocity changes sign from upstream to downstream. The difference in the size of the separation region reveals considerable deviations in the mean and turbulent flow structures and, hence, governs different conditions for sediment entrainment and transport between the separation and reattachment points, X_r, which is ≈3.7D (where D = bedform height).

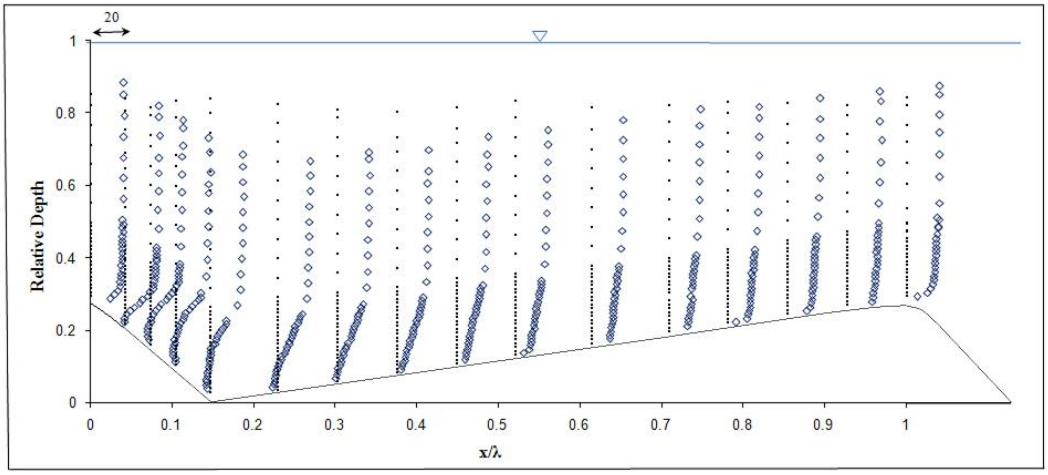

(a)

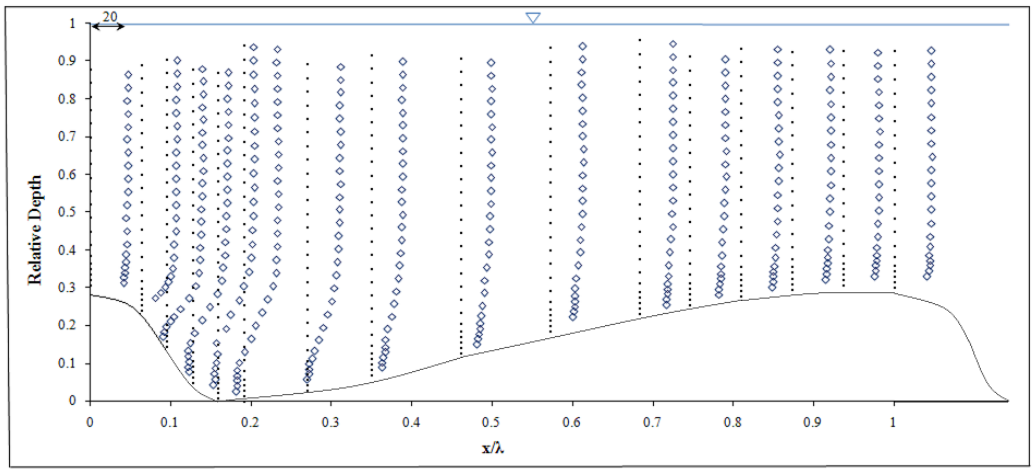

(b)

Figure 2. Non-dimensional velocity profiles (u/u_*) (a) in sharp-crested gravel bedforms and (b) using Bennett and Best's data over one bed form wavelength, λ

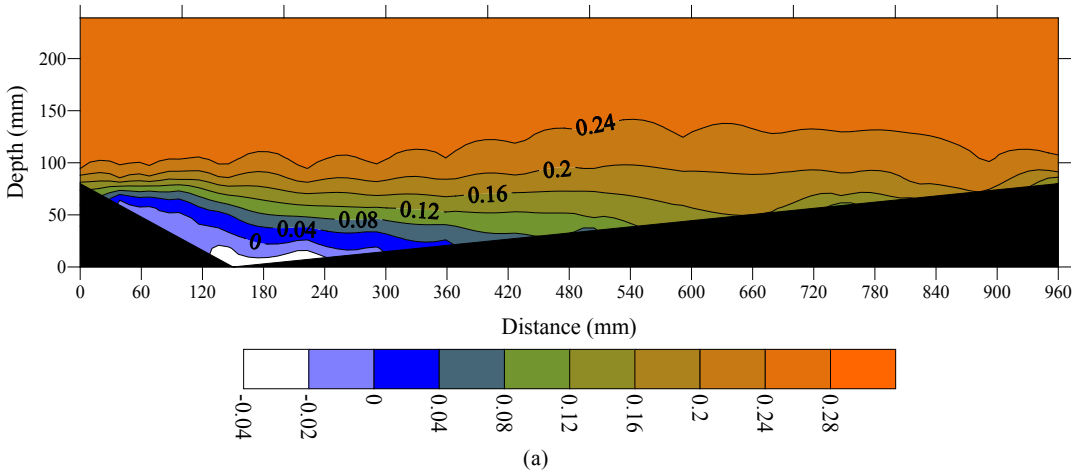

(a)

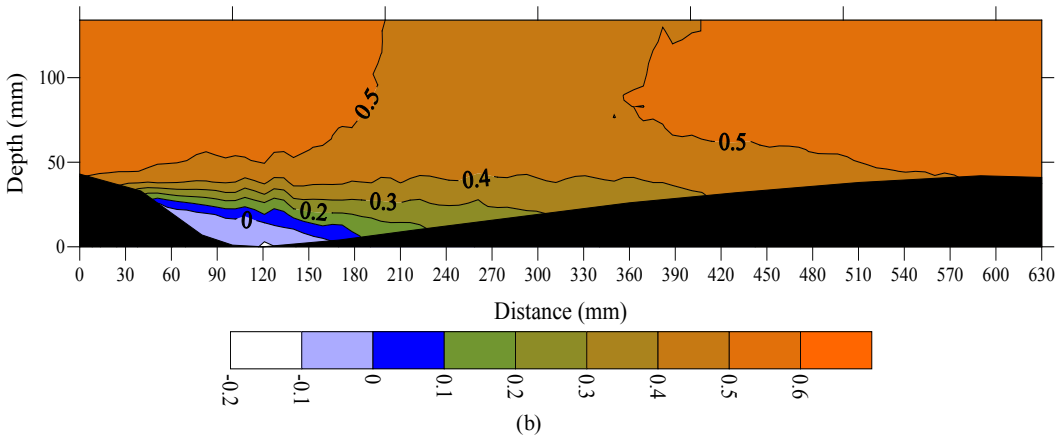

Figure 3. Contour maps of time-averaged downstream velocity ($\overline{u}$(m.s^{-1})) over one bed form wavelength in (a) sharp-crested gravel bedforms and (b) using Bennett and Best's data (1995). Flow is from left to right, color legend is given

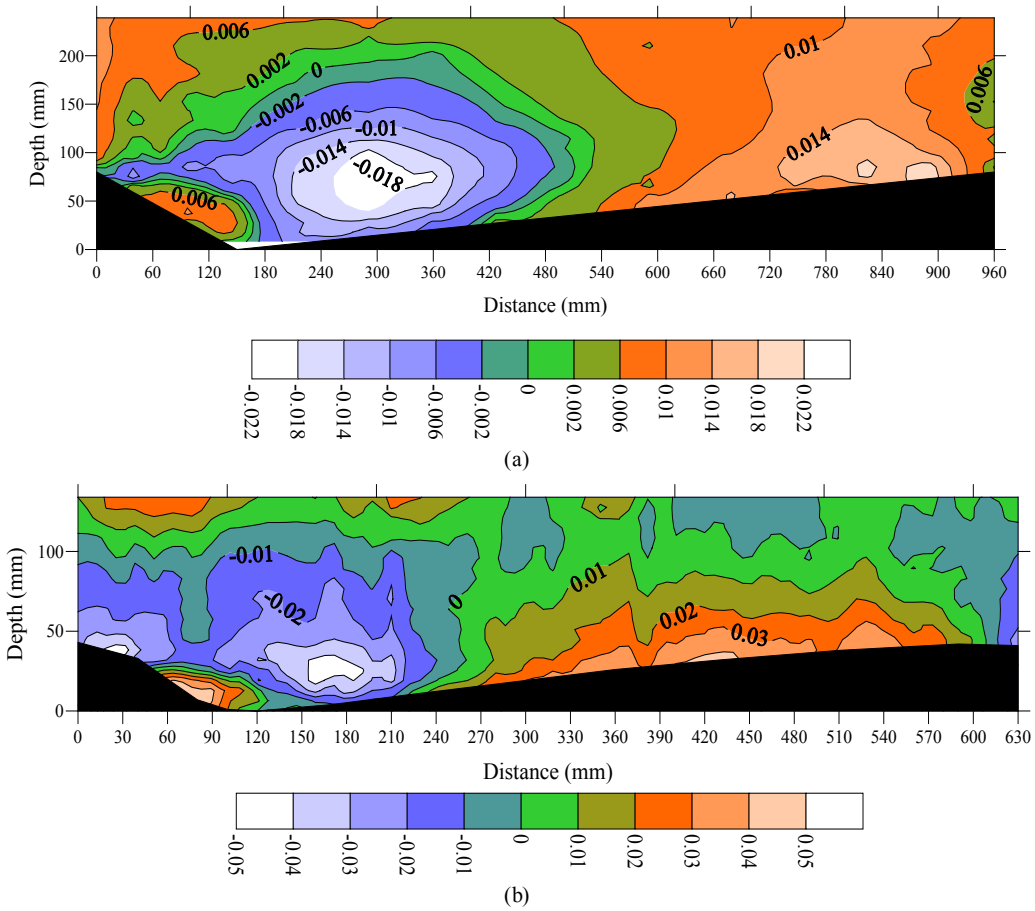

Figure 4. Contour maps of time-averaged vertical velocity ($\overline{w}$ (m.s^{-1})) over one bed form wavelength in (a) sharp-crested gravel bedforms and (b) using Bennett and Best's data (1995). Flow is from left to right, color legend is given

Minimum length of separation was observed in this study in comparison with other studies over smooth or sand bedforms (e.g. 4*D* in the study with *W*/*h*=3.5 and *D*/*L*=0.05[14]; 4.25*D* in the study with *D*/*L*=0.063 and *W*/*h*=3 ([1], Fig.3b); 5.8*D* in the study over the sand dunes with *D*/*L*=0.09 and *W*/*h*=2[19]; 4*D* in the study over smooth dunes with *D*/*L*=0.1 and *W*/*h*=2[20]). However, this finding may be influenced by the weakness of the ADV to make measurements in the separation zone, because most of the other observations of separation zones have been done with LDVs that are capable of resolving much smaller velocity structures.

The experimental data show that the time-averaged vertical velocity over the bedform crest was close to zero. As flow expansion and separation commenced, streamlines were directed towards the bed and significant negative mean velocities (-0.002 to -0.02 m.s^{-1}) occurred just downstream of the crest and downstream of the separation point (Figure 4a,

b). Positive vertical velocities within the separation cell show a strong circulation pattern, especially near the bedform slip-face. Topographic forcing caused accelerating flow over the next bedform stoss, producing positive vertical velocities near the bed.

4.2. Turbulence Intensity and Shear Stress Distributions

Contour maps of the root-mean-squared (RMS) of the downstream velocity (u') in gravel and sand bedforms are shown in Figures 5a and b, respectively. High u' values, up to 0.067 m.s^{-1}, occurred at and just downstream of the reattachment point and they diffused towards the water surface and the bed farther downstream (Figure 5a). The intensity was observed to be prominent downstream of the crest and persisted for a longer distance. Maximum u' values in gravel bedforms were located at a further distance from the bed when compared with those observed over sand dunes by Bennett and Best (1995) (Figure 5b).

High w' values, up to 0.039 m.s^{-1}, occurred inside and above the flow separation zone along the shear layer (Figure 6a) similar to those observed over sand dunes by Bennett and Best (1995) (Figure 6b). Note that w' had behavior similar to that of u', however with smaller values. The region of high w' values (from 0.026 to 0.038 m.s^{-1}) extended from the bedform crest level towards the next crest, completely encapsulating the shear layer produced at the separation zone. Since this region was detached from the bed, the relatively high w' values were not the result of topographic forcing of the flow over the next bedform back but were associated with eddy shedding along the shear layer. Low w' values (from 0.005 to 0.02 m.s^{-1}) were present within the flow separation zone along the bedform slip-face and near the water surface. The turbulence intensity within the boundary layer developed a strong peak at the onset of the adverse pressure gradient along the shear layer originating at the crest.

As expected, the maximum exchange of fluid momentum occurred along the shear layer, where both high u' and w' values were observed. In general, most of the turbulence production occurred in the separated shear layer, where the peak of the stress-intensity profiles was observed. High turbulence intensity indicated a potential for erosion and further along downstream, the turbulence intensity decreased leading to sediment deposition.

The locus of the maximum turbulence intensity was advected along the mean flow streamlines around the separated flow region, bringing turbulent fluid from the free shear layer immediately downstream of the bedform crest towards the bed.

Figure 7 shows the non-dimensional Reynolds shear stress profiles ($-\overline{u'w'}/u^{*2}$) at different stream-wise distances along the downstream direction. Figure 7a indicates that the Reynolds shear stress distribution had features similar to those reported by Bennett and Best[1] (Figure 7b), and Nelson et al.[14], regardless of the magnitude of the bedform lee slope. Ihis shows that the shear stresses at the near-bed surface were smaller than those in the shear layer region. In addition, this figure reveals that the Reynolds stress distribution over much of the bedform is governed by turbulence generated in the free shear layer (outer region) downstream of the separation point at the bedform crest. Nelson et al.[14] found that the maximum values of the Reynolds stress ($\tau = -\rho\,\overline{u'w'}$) over two-dimensional bedforms typically occurred at and just downstream of the reattachment zone, along the shear layer. Reynolds stresses near the bed were somewhat larger than those in the decaying wake above but they were significantly smaller (by nearly an order of magnitude) than those observed in the wake zone over the separation zone.

The present study failed to observe this pattern, in all likelihood because the ADV could not accurately collect data in the internal boundary layer (IBL) region. Figure 8a, which contains a contour map of the spatial variation in Reynolds stress, shows that the maximum τ values (up to 1.37 Pa) occurred both at and just downstream of the reattachment point (y=30mm) as well as along the shear layer extending from the crest level to approximately 0.5L (similar to the results of Bennett and Best (1995), Figure 8b). Additionally, over the lee slope Reynolds stress profiles exhibited a change in slope near the bed (see Figure 7). However, such a change disappeared when the flow moved over the stoss side of the bedform. Furthermore, it was observed that the maximum stresses were located along the shear layer below the crest level (similar to those reported by Bennett and Best,[1]). Zero and slightly negative τ values near the water surface reflected very low shear in this region and the influence of the free-water surface. Nelson et al.[14] observed similar zero and negative τ values and suggested that exact equilibrium flow over the fixed bed forms was not achieved. The shear stress in the layer near the free surface was the lowest and apparently the bedform geometry did not considerably affect this layer.

The high Reynolds stresses confirm that turbulence had greatest values in the separation zone, at the reattachment point and along the shear layer. Although previous studies observed these high turbulence intensities[14], none quantified the magnitude of this turbulence nor did they delineate the morphology and downstream extent of this highly turbulent region.

The weak peak in the shear stress profiles at the bedform crest was due to the development of a local internal boundary layer (IBL) that formed at the point of reattachment and extended up to the bedform crest. Nelson et al.[21] stated that the bed boundary condition induces a thin internal boundary layer that forces the flow by relatively large-scale structures which are ineffective for transporting momentum in the vertical direction. This means that in real flows, one should have the no-slip condition at the bed as a boundary condition. However, for the very rough flows that the authors are investigating there were large velocity fluctuations right down to the point where the mean velocity extrapolated to zero because of the eddies shed by the roughness elements (see Figures 5 and 6). Figure 8 indicates that the correlation coefficient between u' and w' became smaller (not necessarily zero) near the bed.

Figures 3, 5, 6 and 8 show that the high turbulence intensity (Figures 5, 6) and high Reynolds stress (Figure 8) within the inner layer (near the bed) were characterized by low velocity in the recirculation region (Figure 3); whereas the region of outer flow was dominated by a high velocity, low Reynolds stress and turbulence intensity. Accordingly, sediment transport took place in the coherent flow structures characterized by high turbulence intensity and low velocity near the bed.

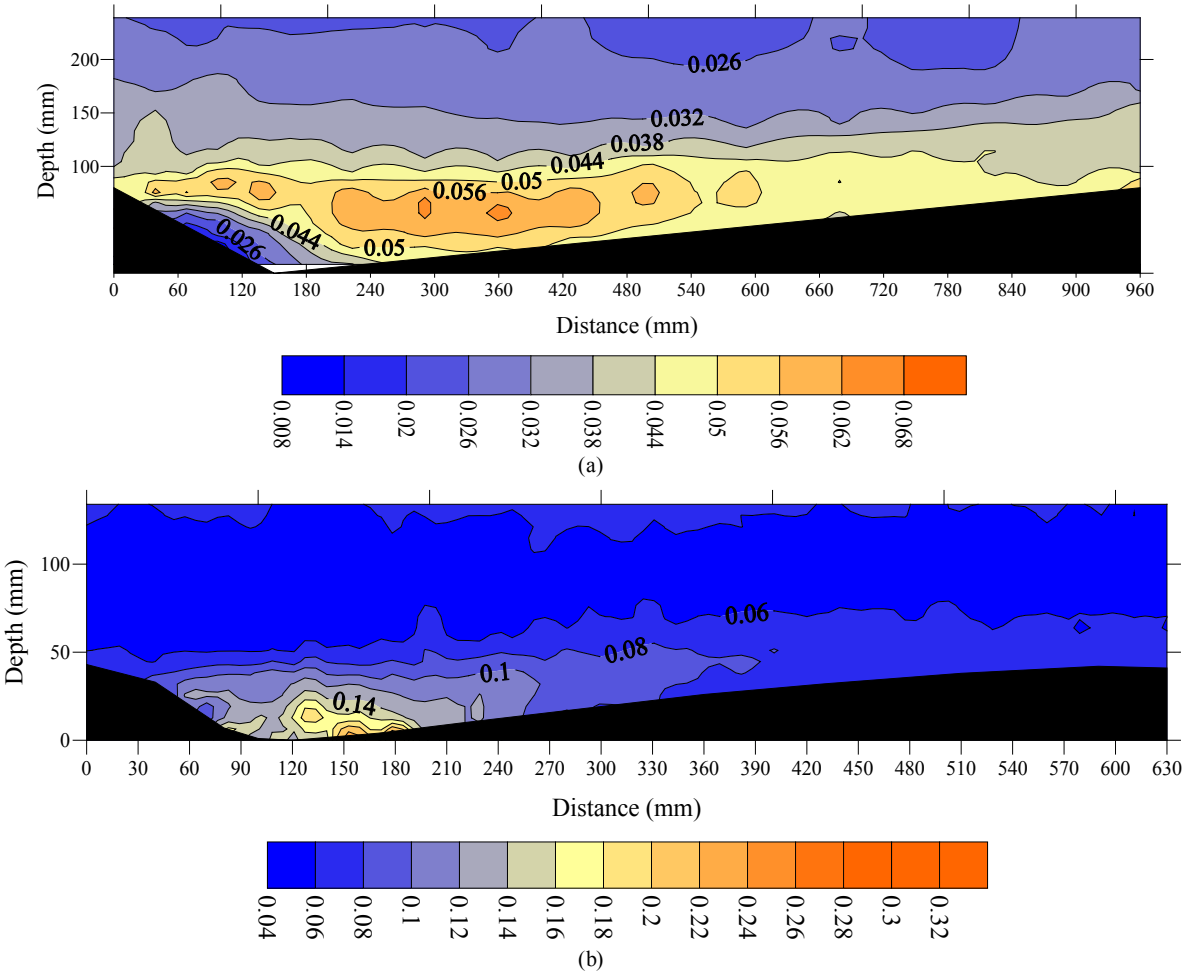

Figure 5. Contour maps of streamwise RMS velocity (u') over one bed form wavelength in (a) sharp-crested gravel bedforms and (b) using Bennett and Best's data (1995). Flow is from left to right, color legend is given

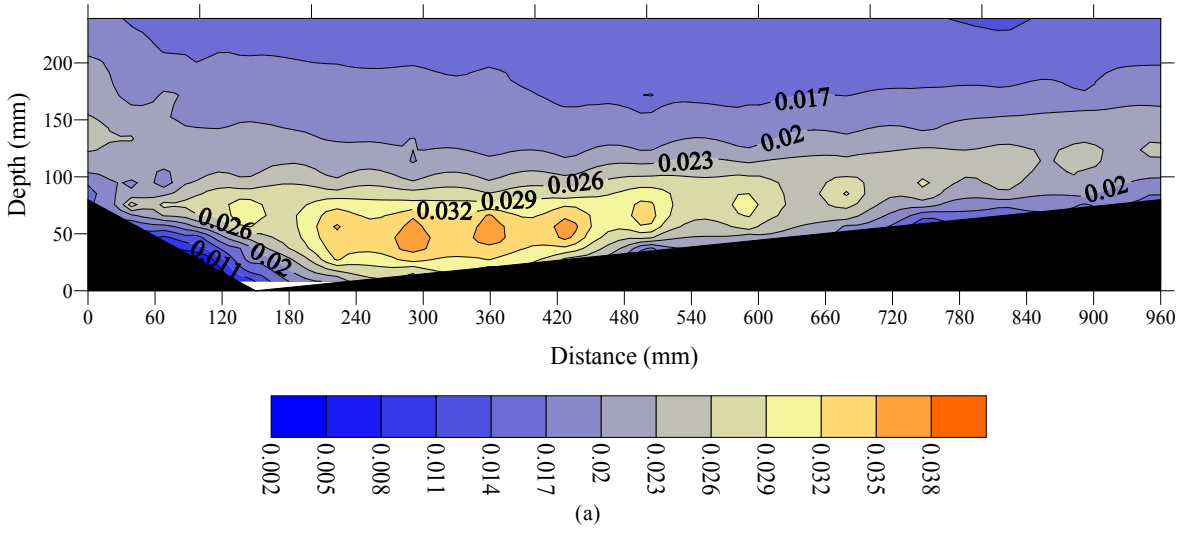

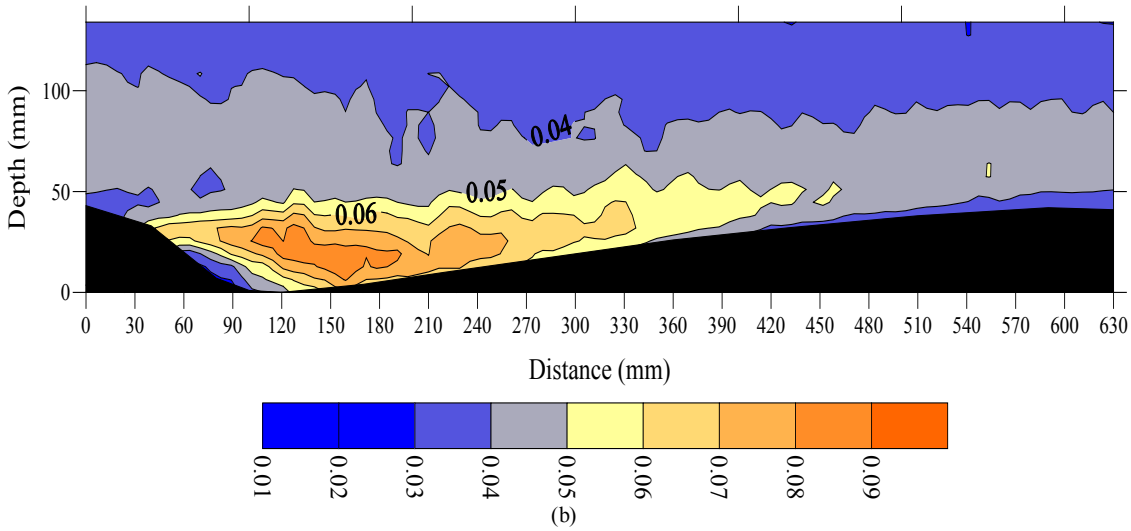

(b)

Figure 6. Contour maps of vertical RMS velocity (w') over one bed form wavelength in (a) sharp-crested gravel bedforms and (b) using Bennett and Best's data (1995). Flow is from left to right, color legend is given

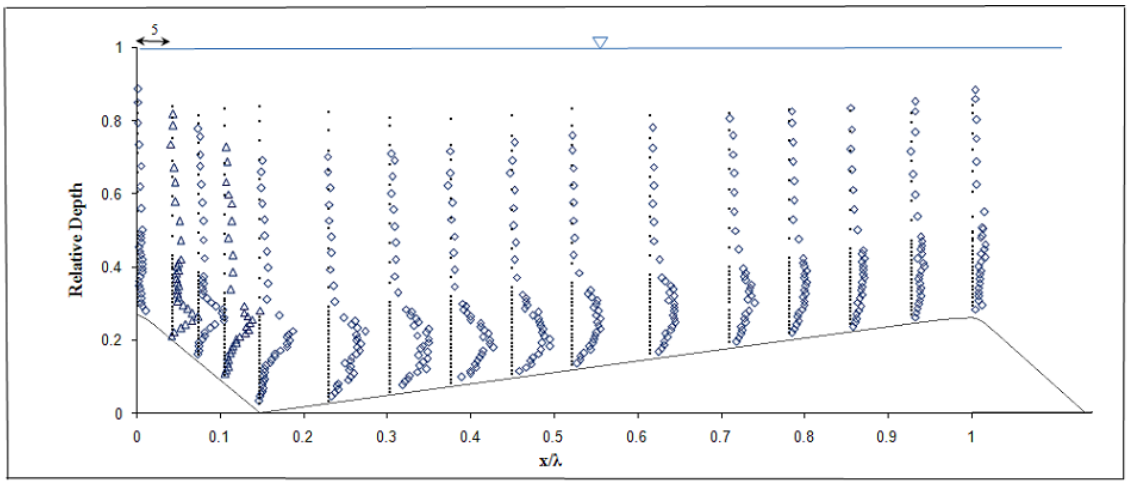

(a)

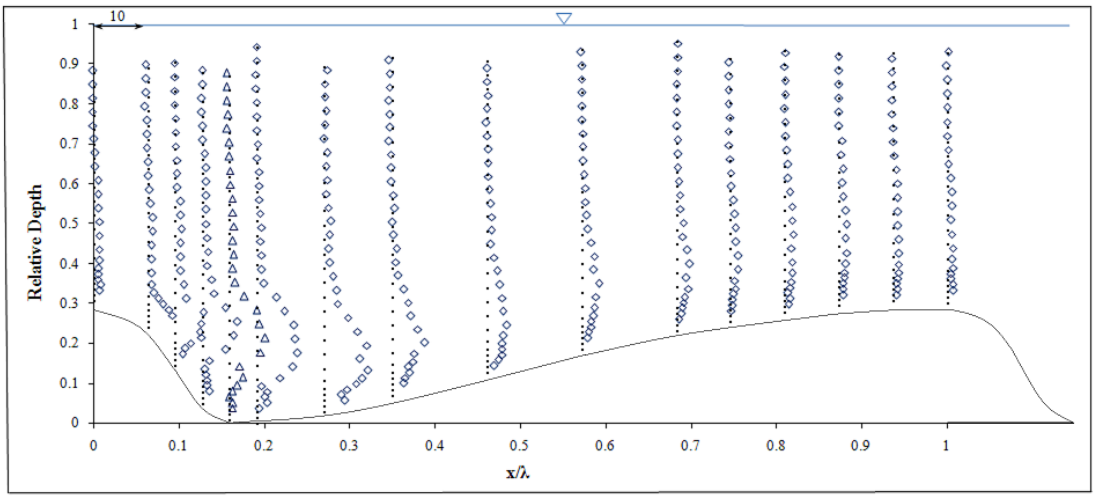

(b)

Figure 7. Non-dimensional Reynolds shear stress profiles ($-\overline{u'w'}/u^{*2}$) (a) in sharp-crested gravel bedforms and (b) using Bennett and Best's data (1995) over one bed form wavelength, λ

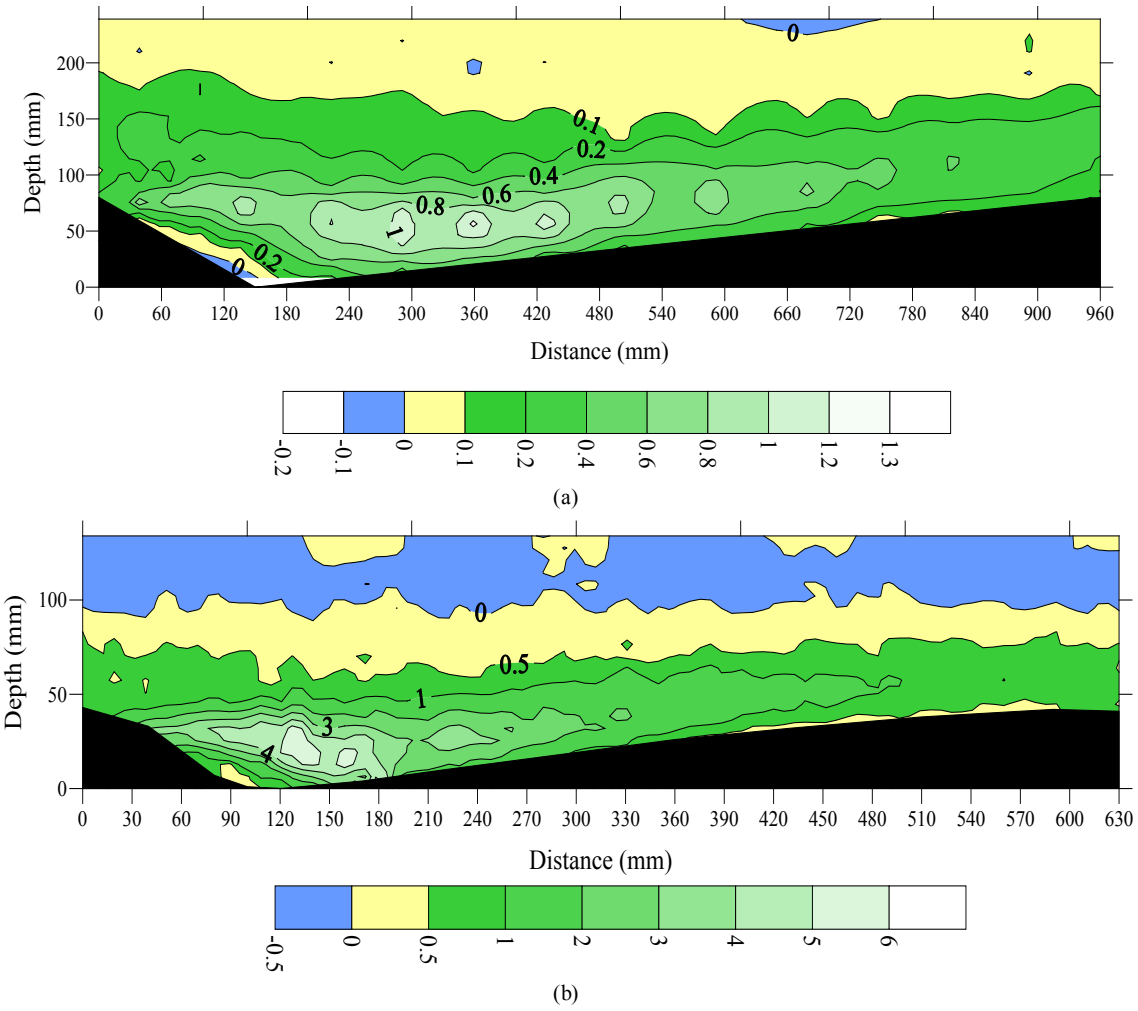

Figure 8. Contour maps of turbulent Reynolds stress ($\tau = -\rho\,\overline{u'w'}$ (N.m^{-2})) over one bed form wavelength in (a) sharp-crested gravel bedforms and (b) using Bennett and Best's data (1995). Flow is from left to right, color legend is given

5. Discussion

The roughness size in Bennett and Best's study (1995) (d_{50} =0.3 mm) was different from that in our study (d_{50}=10 mm), also the geometry of bedforms was different between the two studies. However, Figure 9 shows that in both studies little difference was observed in lee and stoss zones for two studies. The higher values of velocity for sand bed form (Bennett and Best' data) in Fig. 9 were due to higher mean velocity (see Table 1).

The shape of sharp bedform was such that separation did not occur at the crest (highest point) but rather at a brink that was located somewhat downstream. Thus the effective height of the bedform was less and the extent of the separation zone appeared thinner than might have been expected. In addition, the separation zone was smaller because separation was delayed beyond the crest for sharp-crested bedform. The roughness created more mixing of the flow near the bed, therefore, the rougher bed (gravel) yielded lower velocity near the bed. Hence, the separation occurred more readily than that observed in the sand-bed channel. The sharp slope change at the crest of the gravel bedforms forced the separation to occur there.

The results of this study show that the log law can be applied over bedforms, however, it did not work well locally. The log law worked well for spatially-averaged velocity profiles. The difference between calculated shear velocity by a single profile and spatially averaged velocity profiles along a bedform including, stoss, crest and lee zones was considerable. Accordingly, extrapolating spatially-averaged log-law profiles provided the best estimate of bed shear stress for different roughness sizes and bed form geometries.

One may argue for extrapolating the lowest portion of the Reynolds stress profiles but this will give values near zero everywhere since both the streamwise and normal velocities are approaching zero as the bed is approached and viscous stresses increase. Within the separation zone (downstream of crest), in the lee zone, turbulence levels were very high but correlation coefficients were not high as the bed was approached showing the turbulent stress was not useful for determining the local bed shear stress. Therefore, application of the log law could provide a better estimate than the application of Reynolds stress method.

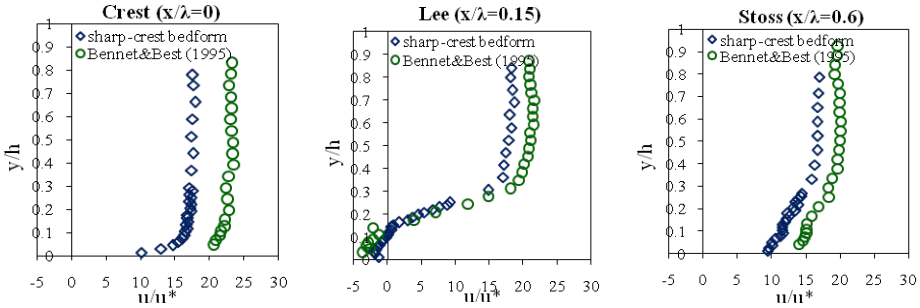

Figure 9. Non-dimensional velocity profiles (u/u_*) in three sections over one bed form wavelength λ (or dune length L)

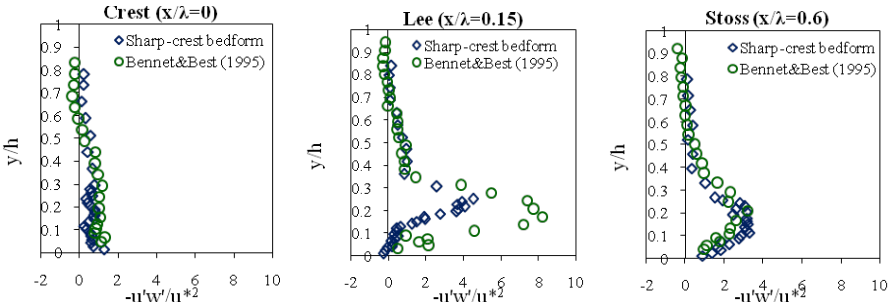

Figure 10. Non-dimensional Reynolds shear stress profiles ($-\overline{u'w'}/u_*^2$) in three sections over one bed form wavelength λ (or dune length L)

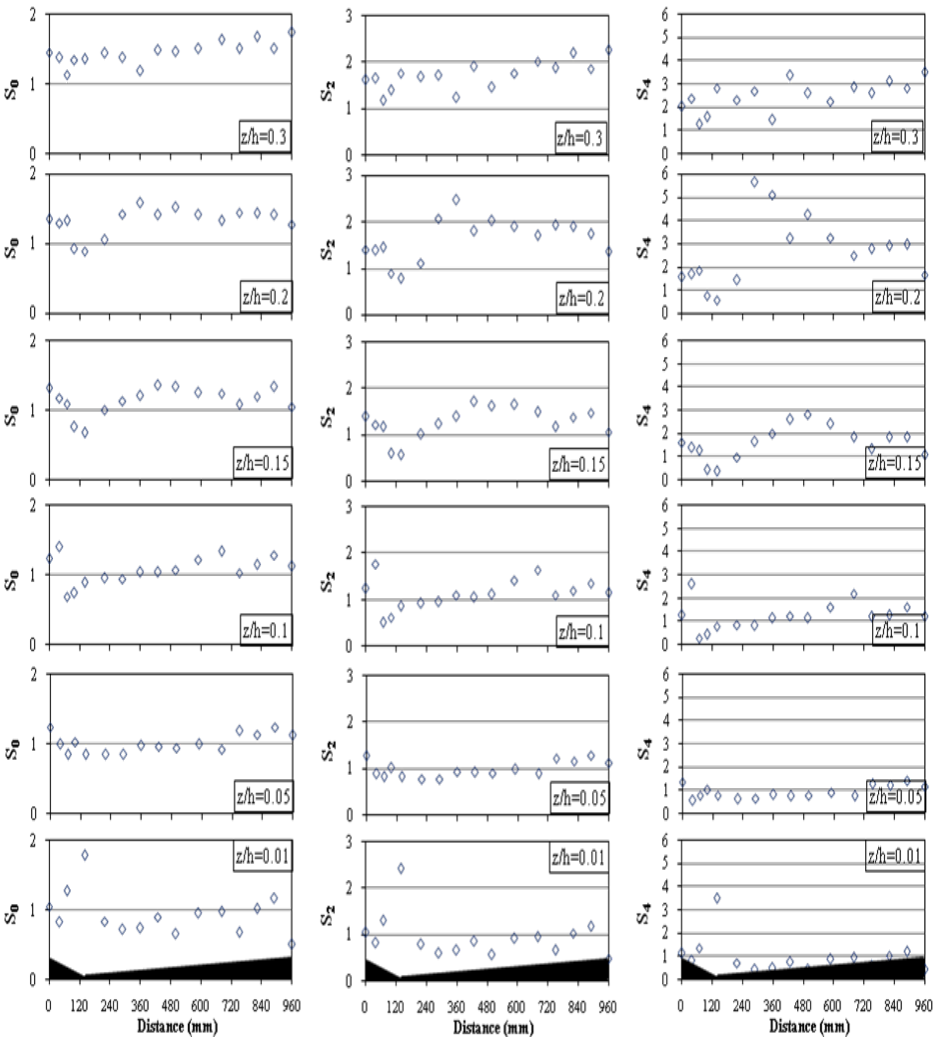

Figure 11. Variation of S_H ($H = 0, 2, 4$) over one dune wavelength (5th and 6th) at six vertical heights

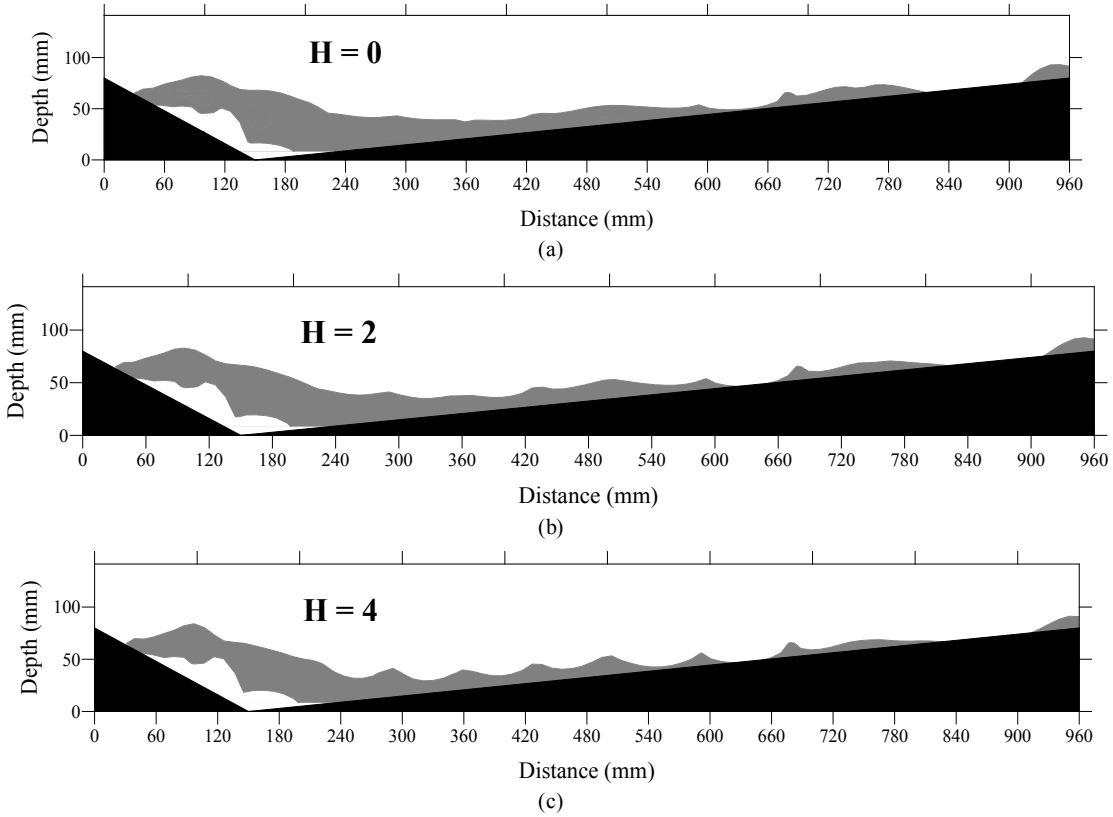

Figure 12. Spatial distribution of the dominant ejection and sweep events for threshold parameter: (a) $H = 0$, (b) $H = 2$, (c) $H = 4$. The White color represents the region of ejection dominance and the grey color represents the region of sweeping dominance

Interestingly, similar distributions of the Reynolds stress (convex form) were observed in stoss and lee sides for different gravel and sand bed forms, the momentum equation ($\partial p/\partial x = \partial \tau/\partial y$) explaining their patterns(see Fig. 10). This equation shows that an increase in longitudinal pressure gradient ($\partial p/\partial x$) causes an increase in vertical Reynolds stress gradient ($\partial \tau/\partial y$). However, a different pattern was observed over the crest region (Fig. 10) which could not be easily described. Although the flow condition was quasi-uniform, the quadrant analysis showed that negative values of Reynolds stress were due to dominant contributions of the outwards and inwards components, while for positive values of Reynolds stress, the sweeps and ejections were dominant events. The relative dominance of sweep and ejection events varied along the sharp-crested gravel bedforms in an oscillatory pattern close the bed, whereas such a pattern was not observed towards the outer layer near the water surface.

To predict the relative dominance of ejection and sweep events, ratios of S_0, S_2 and S_4, were computed at various heights ($z/h = 0.01$; 0.05; 0.1; 0.15; 0.2; 0.3) over the 5th and 6th bedform length and are presented in Figures 11a, b and c. It is observed from these figures that S_0, S_2 and S_4 displayed an oscillatory pattern near the bed. However, in the outer region $z/h > 0.3$ such pattern became weak. It is noteworthy that at the bedform surface ($z/h = 0.01$), the sweep events were dominant throughout the bedform length except at the trough location and at the bedform crest. Starting from the tail end of the bedform, S_H ($H = 0$; 2; 4) decreased up to a length of about $0.2L$ (the reattachment point) and then increased to the trough point indicating the dominance of sweep events in the separation region.

At the level $z/h = 0.05$, for all values of H, sweeps were dominant throughout the bedform length except at the bedform crest and at the end of stoss. Moreover, the maximum value of S_0 occurred at the crest and the maximum value S_2 and S_4 occurred at the stoss at a distance of about $0.8L$ from the tail end of the bedform. At $z/h = 0.1$ for all values of H, sweeps were dominant only within the separation zone, while ejections contributed more over the rest of the bedform length. At $z/h = 0.15$ and $z/h = 0.2$, the sweep events contributed more than the ejection events only at the trough position; over the rest of the bedform ejection events were dominant over the sweep events. The locations of the maximum values of S_0, S_2 and S_4 were shifted upstream and located at a distance of about $0.3L$ from the tail end for $z/h = 0.15$; and $0.2L$ from the tail end for $z/h = 0.2$.

At z/h = 0.3, ejection events were the dominant contributors over the whole bedform length. In fact, this phenomenon was almost similar to that found on a flat surface[22], showing the negligible effect of bottom topographic features away from the boundary.

As the value of the threshold parameter H increased, the region of sweep decreased, implying that in the higher flow

depth, the ejection generated more contribution to the Reynolds stress values. Also, sweep events dominate within the separation zone, at the reattachment point and at the bedform crest (see Figure 12).

6. Conclusions

This paper presented and compared results of the mean velocity, Reynolds stress and turbulence intensities distributions over sharp-crested gravel bedforms with those reported by Bennett and Best (1995) over sand dunes. The comparison of sand and gravel bedforms highlighted that the most important effects occurred in the crest zone; however, stoss and lee zones did not reveal any considerable changes for different Froude numbers and bedform height – to - wavelength ratio, D/λ (or D/L). This finding along the bedforms provided insights to understand the overestimation or underestimation of existing friction factor equations in which the largest relative roughness (d_{50}/h) occurs at crest and the least relative roughness occures at lee.

The spatially-averaged method can improve the prediction of the friction factor over bedforms in rivers. Extrapolating spatially-averaged log-law profiles revealed to be the best estimate of the bed shear stress.

The time-averaged vertical velocity upstream of the sand dune crest was zero or negative near the water surface, whereas it was positive for sharp-crested gravel bedforms.

Maximum values of RMS u over sharp-crested gravel bedforms were located far from the bed when they were compared to those over sand dunes.

The Reynolds stresses were zero or negative near the water surface over sand dunes, while they were positive over sharp-crested gravel bedforms.

The variation of hole size (H) from 0 to 4 did not affect considerably the occurrence of sweep and ejection events along lee and stoss.

ACKNOWLEDGEMENTS

The authors wish to acknowledge Professor Best for giving his valuable data set and Professor Carling to read the manuscript.

Notation

The following symbols are used in this paper:

d_{50}	Median diameter of sediment particles;
d_{16}	16% finer particle diameter;
d_{84}	84% finer particle diameter;
Fr	Froude number;
g	Gravitational acceleration;
h	Water depth;
H	Hole size ;
D	Bed form or sand dune height;
λ	Bed form wavelength;
L	Sand dune length;
Q	Flow discharge;
Re	Reynolds number;
Re^*	Particle Reynolds number;
R_h	Hydraulic radius;
U	Depth-averaged velocity;
u	Mean-point velocity in the stream-wise (or longitudinal) direction;
u'	Root-mean-squared of streamwise (or longitudinal) velocity fluctuations;
u_i	Instantaneous velocity in the stream-wise (or longitudinal) direction;
u^*	Shear velocity;
$\overline{u}$	Mean-point velocity;
$\overline{u}_C$	Maximum velocity;
v	Mean-point velocity in the lateral (or transversal) direction;
v'	Root-mean-squared of lateral velocity fluctuations;
v_i	Instantaneous velocity in the lateral (or transversal) direction;
w	Mean-point velocity in the vertical direction;
w'	Root-mean-squared of vertical velocity fluctuations;
w_i	Instantaneous velocity in the vertical direction;
x	Distance from the flume entrance;
X_r	The length of flow separation;
z	Distance from the bed;
v	Kinematic viscosity;
ρ	Mass density of water;
σ_g	Geometric standard deviation;
W/h	Aspect ratio;

REFERENCES

[1] Bennett, S. J., and Best, J. L., 1995, Mean flow and turbulence structure over fixed, two-dimensional dunes: Implications for sediment transport and bed form stability., Sedimentology, 42(3): 491–513.

[2] Carling, P. A., 1999, Subaqueous gravel dunes., J. Sediment. Res., 69: 534–545.

[3] Carling, P. A., Richardson, K., Ikeda, H., 2005, A flume experiment on the development of subaqueous fine-gravel dunes from a lower-stage plane bed., Journal of Geophysical Research, Vol. 110, F04S, 05-15 pp.

[4] Dinehart, R. L., 1989, Dune migration in a steep, coarse-bedded stream., Water Resour. Res., 25: 911–923.

[5] Dinehart, R. L., 1992a, Evolution of coarse gravel bed forms: field measurements at flood stage., Water Resour. Res., 28: 2667–2689.

[6] Dinehart, R. L., 1992b, Gravel-bed deposition and erosion by bed form migration observed ultrasonically during storm flow, North Fork Toutle River, Washington., J. Hydrol., 136:

51–71.

[7] Engel, P., 1981, Length of flow separation over dunes., J. Hydraul. Div., ASCE, 107(HY10): 1133–1143.

[8] Williamson, A., Feyer, A. M., Rivalenti, G., Mazzucchelli, M., Girardi, V. A. V., Cavazzini, G., Finatti, C., Barbieri, M. A., Teixeira, W., Villard, P., Kostaschuk, R., 1998, The relation between shear velocity and suspended sediment concentration over dunes: Fraser Estuary, Canada., Marine Geology, 148(1): 71-81(11).

[9] Frank, A., and Kocurek, G., 1996, Toward a model for airflow on the lee side of aeolian dunes., Sedimentology, 43: 451–458.

[10] Walker, I. J., and Nickling, W. G., 2002, Dynamics of secondary airflow and sediment transport, over and in the lee of transverse dunes., Progress in Physical Geography, 26(1): 47-75.

[11] Tsoar, H., 1985, Profiles Analysis of Sand Dunes and Their Steady State Signification., Geografiska Annaler, Series A, Physical Geography,67(1/2): 47-59.

[12] McLean, S. R., Nikora, V. I., Coleman, S. E., 2008, Double-averaged velocity profiles over fixed dune shapes., Acta Geophysica, 56(3): 669-697.

[13] Franca, M. J., Ferreira, R. M. L., Cardoso, A. H., Lemmin, U., 2010, Double-average methodology applied to turbulent gravel-bed river flows., In River Flow edited by Dittrich, Koll, Aberle and Geisenhainer. ISBN 978-3-939230-00-7, 59-65.

[14] Nelson, J. M., McLean, S. R., Wolfe, S. R., 1993, Mean flow and turbulence over two-dimensional bed forms., Water Resour. Res., 29: 3935–3953.

[15] McLean, S. R., Wolfe, S. R., Nelson, J. M., 1999, Spatially averaged flow over a wavy boundary revisited., Journal of Geophysical Research, 104(C7): 15,743-15,753.

[16] Lu, S. S., and Willmarth, W. W., 1973, Measurements of the structure of the Reynolds stress in a turbulent boundary layer., J. Fluid Mech., 60: 481–511.

[17] Nezu, I., and Nakagawa, H., 1993, Turbulence in open channel flow., IAHR monograph, A. A. Balkema, Rotterdam, The Netherlands.

[18] Fedele, J. J., and Garcia, M. H., 2001, Alluvial roughness in streams with dunes: A boundary-layer approach. River, Coastal and Estuarine Morphodinamics., Edited by Seminara G. and Blondeaux P., Springer; 37-60.

[19] Ojha, S. P., and Mazumder, B. S., 2008, Turbulence characteristics of flow region over a series of 2-D dune shaped structures., Advances in Water Resources, 31: 561–576.

[20] Mazumder, B. S., Pal, D., Ghoshal, K., Ojha, S. P., 2009, Turbulence statistics of flow over isolated scalene and isosceles triangular-shaped bed forms., Journal of Hydraulic Research, 47(5): 626–637.

[21] Nelson, J. M., Schmeeckle, M. W., Shreve, R. L., McLean, S. R., 2001, Sediment entrainment and transport in complex flows. River, Coastal and Estuarine Morphodinamics; Edited by Seminara G. and Blondeaux P., Springer: 11-35.

[22] Nakagawa, H., and Nezu, I., 1977, Prediction of the contribution to the Reynolds stress from bursting events in open-channel flows., J. Fluid Mech., 80(1): 99–128.